Chapter 11

Atmospheric Fluctuations

Michael Bremer

bremer@iram.fr

IRAM, 300 rue de la Piscine, F-38406 Saint Martin d'Hères, France

11.1 Introduction

We have already encountered the effects of atmospheric absorption in the lecture by Michel Guélin (Chapter 10). Even under low opacity conditions, observations can be difficult or impossible due to atmospheric phase fluctuations. In principle, integration of an interferometric signal is like the adding up of vectors. The amplitude is the length of a vector, and its orientation is given by the phase. Errors in the phase will cause part of the amplitudes to cancel each other out according to Eq. 11.1

$$\overline{V_{ij}^m} = V_{ij} \exp\left(-\sigma_\phi^2/2\right) \tag{11.1}$$

where V_{ij} are the ideal visibilities, $\overline{V_{ij}^m}$ the integrated ones, and σ_ϕ the phase noise in radian (assuming a Gaussian noise distribution).

If our eyes were sensitive in the millimeter range with a resolving power of some arc seconds, we would not only see a luminous sky where sources are difficult to make out on the background: we would notice refracting bubbles of sizes between some centimeters to several kilometers drifting with the wind, merging, separating and distorting the view behind them. It is water vapor which has not attained the concentrations necessary for cloud formation, and mixes badly with dry air. Even in the case of low opacity and a sky clear for human perception, these distortions - which are shifts and tilts in the incoming phase front - can be so important that they make observations impossible.

In this lecture we will study the physics behind this effect and possible ways to correct for it which have become available in recent years.

The phases of a wave front that reaches ground-based observatories have been modified by their journey through refractive index variations in the Earth's atmosphere. The instrument itself has no way to tell

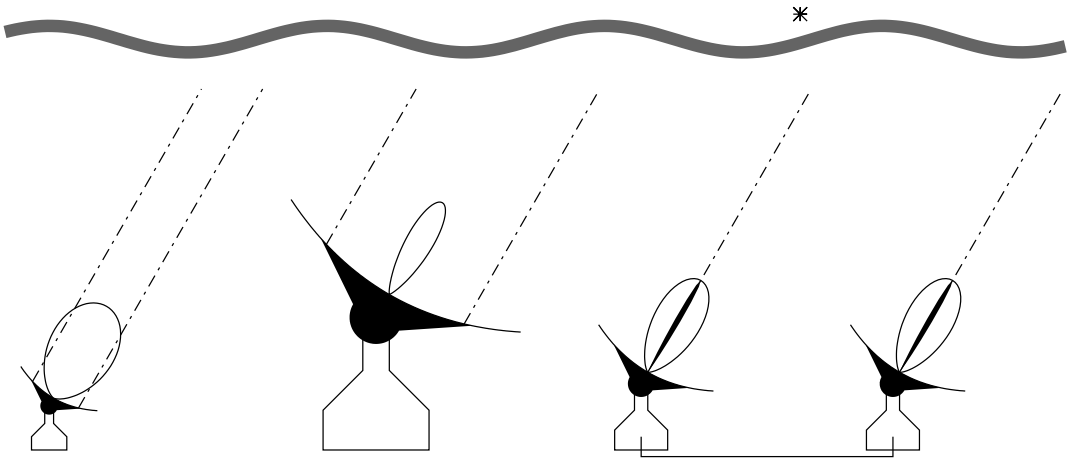

Figure 11.1: Two single dish radio telescopes and one synthesis array observing a source. Angular resolution and the effects of atmospheric turbulence increase with the diameter of an instrument. An interferometer's synthesized beam has the same problems that a single dish with a projected baseline's diameter would experience.

which part of the phases are due to valuable structure in the astronomical source and which part was caused during the last kilometers in front of the telescope.

As a result, the apparent position of a point source keeps moving, so that details of an extended source become blurred ("seeing"). The perturbations become progressively decorrelated with increasing separation between two lines of sight.

Depending on turbulence scale, wavelength and telescope size, a ground-based observer will be confronted with different effects. To some extent, one can reduce unwanted perturbations by choosing an observatory's site carefully. But there are always some days which are better than others.

- If the telescope diameter is much larger than a typical turbulence cell and if phase shifts over a turbulent cell are less than 1 radian, one works in the **diffractive** regime: some power is scattered into an error beam, but the diffraction limited resolution of the instrument is conserved. These conditions can be found for very long baseline interferometry at cm wavelengths under good conditions.
- In the **refractive** regime, the turbulence cells are much larger than the telescope so that the whole image seems to move around. Phase shifts can be several radians. *This is the case we have to cope with at the Plateau de Bure interferometer.*
- In the **intermediate** case, one gets speckles on short integration times which average into an image convolved with a seeing disk (an effect well-known to optical and near infrared observers).

For a small radio telescope, the phase noise passes unnoticed (Fig.11.1). Its beam size is bigger than the apparent position shifts induced by seeing, and the ray paths leading to the opposing outer edges of the reflector will not differ much. For a big single dish, the effect can become noticeable: under unstable conditions, a source may wander in and out of the beam, disturbing not only the observations of the target of interest but also pointing and focus. An interferometer suffers even more from seeing because the distances between individual antennas are large. This has the double effect of making the synthesized beam smaller and of increasing the differences in the atmospheric turbulence pattern between the optical paths. In the optical and near infrared, it is the dry atmosphere which causes the phase shifts. In the centimeter radio range, it is the tropospheric water vapor and the ionospheric plasma irregularities, and mainly water vapor in the millimeter radio range.

The interest of interferometric phase correction is to determine and remove the atmospheric phase noise. Each individual antenna has to correct a time variable "piston" in the incoming wave front, which is the equivalent of adaptive optics for the synthesized dish.

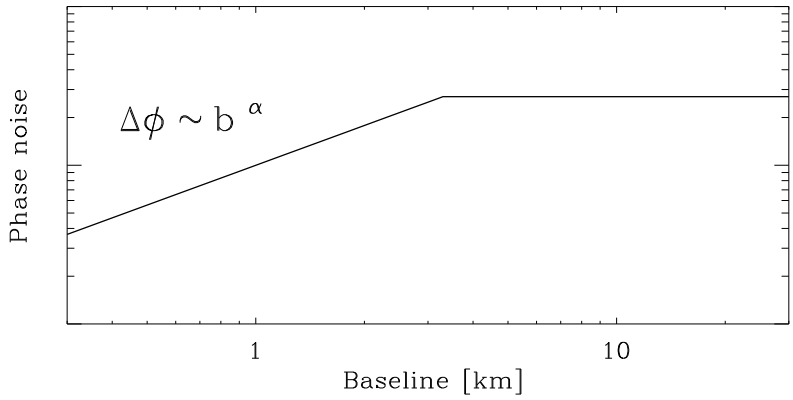

Figure 11.2: Atmospheric phase noise as a function of baseline length. The position of the break and the maximum phase noise are weather dependent.

Most of the water vapor is confined to the troposphere (<10 km) with an exponential scale height of 2 km. Its molecular weight is 18.2 g/mol so that it has the tendency to rise above dry air (28.96 g/mol). Our planet retains the water vapor due to the negative vertical temperature gradient in the troposphere, and the fact that H_2O is close to the transition points to liquid and solid under terrestrial pressure and temperature conditions. Venus is an example for a planet with a hot troposphere (extreme CO_2 and H_2O greenhouse effect) who lost most of its water long ago.

Under Earth's environmental conditions, water vapor mixes badly with dry air and tends to form bubbles with sizes up to several kilometers, which are broken up by turbulent motions. When choosing high and dry sites for millimeter astronomy, one must keep in mind that high phase noise can be induced even by low amounts of precipitable water.

Parameters that influence interferometric phase noise strongly are:

- wind speed,
- projected baseline length,
- the time of the day (nights are typically more stable due to the missing solar energy input to turbulence),
- topographic effects, e.g. the turbulent wakes of mountains.

The leveling off of the phase noise on a high, constant value corresponds to the outer scale size of the turbulence, where the fluctuations along two lines of sight become totally decorrelated, i.e. as bad as they can possibly get (Fig. 11.2). Increasing the baselines will not increase the phase noise any more, and this is why very long baseline interferometry can work.

In the following, some fundamentals about turbulence will be explained, and how one can analyze the properties of a turbulent atmosphere. Possible methods to monitor the phase fluctuations will be discussed, with emphasis on the phase monitoring system on the Plateau de Bure. Some examples with observational data will be presented, demonstrating its benefits and current limitations.

11.2 Hydrodynamical basics of turbulent motion

Turbulence has its origin in the non-linearities of the hydrodynamical equations of motion. These equations are not derived from first principles, but present the easiest consistent way of describing the motion of compressible (gases) or incompressible (liquids) media. Given the complexity of observed hydrodynamical phenomena (white water rivers, curling smoke, ...) it was doubted for more than a century if the equations could really be as simple as given below.

Scepticism was nourished by the fact that some stationary (i.e. time invariant) solutions were mathematically valid but not observed experimentally, which can be understood today by checking the solutions for their stability. It is an interesting fact that stationary solutions are *not* always the most stable ones – this assumption might appear "natural", but is in fact quite misleading. To find out under which conditions one has to expect turbulence, we must have a closer look into the equations of hydrodynamics.

In a free flow (i.e. no outer confinements like tubes) and under sub-sonic conditions, one can treat air as an incompressible medium. This allows to use the Navier-Stokes equations which describe such a medium with viscosity (Eq. 11.2).

$$\underbrace{\frac{d\vec{V}}{dt}}_{1.} + \underbrace{\frac{grad\, P}{\rho}}_{2.} + \underbrace{grad\, U}_{3.} - \underbrace{\frac{\eta}{\rho}\Delta\vec{V}}_{4.} = 0 \tag{11.2}$$

The respective terms describe:

1. This part is the complete derivative in time, containing non-linear terms:

$$\frac{d\vec{V}}{dt} = \frac{\delta\vec{V}}{\delta t} + \left(\vec{V} grad\right)\vec{V} = \frac{\delta\vec{V}}{\delta t} + \underbrace{\frac{1}{2}\, grad\left(\vec{V}\cdot\vec{V}\right)}_{kin.\ Energy} - \underbrace{\vec{V}\times\left(\vec{\nabla}\times\vec{V}\right)}_{Vortices} \tag{11.3}$$

2. The pressure term describes the reaction to external forces, and is related to density and temperature through the equation of state.

3. External forces, described by the gradient of a Potential U. This form makes it easier to include this term into the others. We are interested here in cases where U is constant in good approximation, so we can leave this term out in the following.

4. Energy dissipation. Viscous terms, with the Laplacian operator $\Delta = \nabla^2 = div\ grad$. The material constant η is the viscosity coefficient for incompressive media (there is a term with a second coefficient for compressive media, but it can be neglected here).

To solve Equation 11.2, one needs:

- the equation of state for the gas,
- the conservation of mass and energy,
- the boundary conditions.

We will not have to deal with these equations directly. If you have to solve them for some reason: There is a whole class of numerical methods and library codes in the literature, which avoid non-evident pitfalls concerning different coordinate systems and numerical stability. For the current discussion, we are only interested in the question of similarity.

Flow problems resemble each other for certain combinations of flow velocity, spatial dimension and viscosity. This allows to predict the general properties of a hydrodynamic system (and if it is turbulent or not) from small models or other well-studied cases where the geometries are the same. It is convenient to change to dimensionless equations by expressing lengths and velocities in units of the system's typical length scale l_0 (e.g. the size of an obstacle) and the unperturbated flow velocity V_0.

One obtains not only $V' = V/V_0$ and $l' = l/l_0$, but must change all other units which are combinations of the two: $t' = t \cdot v_0/l_0$, $\rho' = \rho \cdot l_0^3$ and $P' = P \cdot l_0^3/v_0^2$. As a result, we get the dimensionless equation Eq.11.4:

$$\frac{dV'}{dt'} + \frac{grad\, P'}{\rho'} - \frac{1}{Re}\Delta V' = 0 \tag{11.4}$$

Medium	η [g/cm s]	$\nu = \eta/\rho$ [cm^2/s]
Water	0.010	0.010
Air	0.00018	0.150
Alcohol	0.018	0.022
Glycerin	8.5	6.8
Mercury	0.0156	0.0012

Table 11.1: Examples for viscosity and the kinetic viscosity η/ρ various media at 20°C (adapted from [Landau & Lifshitz 1959]). The viscosity changes little with altitude, so that the density dependency of ν dominates and satellites above $\approx$ 300 km altitude experience a non-turbulent, laminar flow.

which contains **Reynold's number** $Re = l_0 \cdot V_0 \cdot \rho/\eta$. It determines the relative influence of the energy dissipating term relative to the non-linear turbulent term. A high Reynold's number will reduce the effect of $\Delta V'$, so that turbulence will develop. Each problem has its specific **Critical Reynold's number** Re_c, which lies typically between 10 and 100. For a given geometry and a $Re > Re_c$, no stable solution exists (e.g. Figure 41-6 from [Feynman et al. 1964]).

With Eq.11.4 and the viscosities from Tab.11.1, we find that for ambient conditions, wind moving faster than 1 cm/s hitting an obstacle bigger than 1 cm generates a turbulent flow. A house (10 m) in a 10 m/s wind has $Re \approx 6 \cdot 10^6$, mountains $Re \approx 1 \cdot 10^9$.

This means that turbulence is something quite common in our environment. In our daily life, we encounter many turbulent systems which defy detailed prediction: leaves of wind-moved trees, eddies in flowing water, the structure of clouds, to name only a few. All these effects are non-linear and will never repeat themselves exactly, although their parameters stay within certain limits.

It may be surprising that these phenomena have been neglected by classical physics for centuries, to become finally popular in the wake of chaos theory and the development of powerful computers. One reason for this was surely the problem of repeating an experiment with inherent chaos exactly, and the sheer bulk of work for doing the calculations. Linear physics were favored not because they are more abundant in nature, but because they were easier to understand and reproduce.

Even chaos theory has a hard time with the atmosphere. The famous "strange attractors" which describe non-repetitive curves in solution spaces are not very useful for turbulence, because one is not sure if the number of solution space dimensions is finite or not in this case.

Meteorology is a well-known (and sometimes notorious) example for predictions of a non-linear system. In spite of a network of measurement stations and satellite data, boundary conditions are not known precisely enough for long term forecasts. This is the famous "butterfly effect": A butterfly moving its wings in South America may change the weather in Europe six months later.

But don't start hunting butterflys to prevent storms right now: this example only illustrates that non-linear systems do not obey the "small cause - small effect" rule of linear physics but a rather imprecise "small cause at the right place may have a big effect" rule. So it could be a butterfly, a spoken word, a thought, or a tree falling in a forest, or all of them together that may tip a balance.

For all practical applications, the interactions are too complex to backtrack the cause – but nevertheless, the history that makes a leaf move right now in a unique way outside your window contains somewhere the gravitational pull of faraway galaxies, and your mere presence will leave traces in the turbulent structures all over the universe (no liabilities implied, fortunately).

A small perturbation may set off a non-linear cause-and-effect chain, but this is only because a turbulent system can have multiple macroscopically different states without violating the conservation of energy. Using a statistical approach, we will now discuss turbulence's energy distribution on different scale sizes. This is an important step to understand how atmospheric parameters (including phase noise) change with time and distance.

11.3 Statistical properties of turbulence

We start with a simple model of turbulence. It must explain why the scale size of the finest turbulence structures becomes smaller and smaller with increasing Re, and should allow to treat the finest details in

a homogeneous way. It cannot explain why certain structures form and not others, but it describes the average flow of energy across the scale sizes of turbulence.

- Kinetic energy enters the medium on large scales, in the form of convection or friction on an obstacle (**energy range**).
- The energy is transferred towards smaller scale sizes over eddy fragmentation, while the Reynolds number decreases (**inertia range**).
- The smallest eddies have sub-critical *Re*'s, dissipate heat, and are stable (**viscous range**).

[Kolmogorov 1941] advanced a hypothesis for high ($Re > 10^6 - 10^7$) Reynold's numbers, postulating that turbulence in the inertia range was determined only by one parameter ϵ (kinetic energy converted to heat by viscous friction per unit time and unit mass). In the viscous range, it would only depend on ϵ and the already discussed viscosity η. This model treats cases like the seemingly amorph eddies-within-eddies part in the Fig.41-6 (d),(e) (from [Feynman et al. 1964]). As we have derived in the previous section, (d) and (e) are indeed the cases to be expected in the troposphere.

The inertia range is interesting for us because it corresponds to spatial dimensions of some meters to 2-3 kilometers, i.e. the baselines of the PdBI fall into this range.

For the mathematical treatment of highly developed turbulence, one can use a formalism based on random variations.

Most "classical" statistics represent a given distribution of probability (binomial, Poisson, Gaussian, ...) around a most likely measurement value. For atmospheric parameters like e.g. temperature and wind velocity, we must make a more general approach: the most likely measurement values vary with time and space, which means they can be represented by *non-stationary random processes*. The classical average and its variation are not very useful to describe these systems.

An instrument for the characterization of non-stationary random variables are *structure functions*, which were first introduced by [Kolmogorov 1941]. A scalar structure function has the form given in Eq.11.5,

$$D_f(x_i, x_j) = \overline{(f(x_i) - f(x_j))^2} \tag{11.5}$$

i.e. a function $f(x)$ is measured at the positions x_i and x_j, squared and averaged over many samples to obtain a $D_f(x_i, x_j)$. When the average level of f changes, the average differences between $f(x_i)$ and $f(x_j)$ stay constant.

The structure function formalism can even be used to describe vector parameters like the turbulent wind velocity, in this case one simply needs 3×3 tensors of structure functions for their description. We won't need tensors in the following discussion, however. The detailed mathematical formalism of random fields would be too much for this course (see [Tatarski 1971] for details). We will only discuss the basic concepts and their application to phase shifts.

Real atmospheric parameters are functions of time and space. For time dependency, Taylor's hypothesis of frozen turbulence has been quite successful (Eq.11.6). It states that the pattern of refractive index variations stays fixed while it is moving with the wind.

$$f(x, t + t') = f(x - V_{al} \cdot t', t) \tag{11.6}$$

This means that for the structure functions, one can either measure at two different sites simultaneously or measure in one place and compare different times. Time-like structure functions are often easier to determine because the sampling is continuous and instrumental effects are reduced by averaging. The velocity V_{al} is also called "Velocity aloft" and can differ notably from measurements of a ground-based meteorological station: wind speeds increase with altitude and change direction due to the diminishing effect of ground friction.

For two measurement points which are a distance r apart from each other, one finds that the structure functions of many atmospheric parameters (temperature, refractive index, absolute wind velocity, ...) obey a $r^{2/3}$ power law. This law can be derived from the theory of random fields, but the easiest way is as follows:

Consider a velocity fluctuation δV_r (where δV_r may be large) which occurs on a scale size r and a time $t = r/\delta V_r$:

- its energy per mass unit is $\propto (\delta V_r)^2$
- The energy per mass and time: $\epsilon \propto \delta V_r^2/t = \delta V_r^3/r$
- Stationary transport of this energy from large to small scale sizes, where it is finally dissipated
- Approximately, $D_{rr}(r) = \overline{(V(r_l + r) - V(r_l))^2}$ is dominated by eddies of size r, i.e. $D_{rr}(r) \approx (\delta V_r)^2$
- Therefore, the formula for intermediate scale sizes is:

$$D_{rr}(r) \propto (\epsilon \cdot r)^{2/3} \tag{11.7}$$

For a thin layer, refractive index fluctuations and phase fluctuations are identical. This is the *thin screen approximation.*

$$D_\varphi(r) = C \cdot (\epsilon \cdot r)^{2/3} \tag{11.8}$$

In a thick turbulent layer, the phase front encounters multiple refractive index fluctuations and the power law index changes. This problem can be solved by analyzing the irregular refracting medium over its Fourier transform. After [Tatarski 1961], the spectral density of the function

$$D(r) = r^p \tag{11.9}$$

with $0 < p < 2$ is in the three dimensional case

$$F'(\kappa) = \frac{\Gamma(p+2)}{4\pi^2} sin(\pi p/2)\kappa^{-(p+3)} \tag{11.10}$$

An important condition is that the fluctuations must have an outer limit, i.e. that the power law does not increase indefinitely. To get the phase fluctuations from the refractive index spectrum, we take

$$D_\varphi(r) = 4\pi \int_0^\infty [1 - J_0(\kappa r)]F'(\kappa)\kappa d\kappa \tag{11.11}$$

with the Bessel function J_0 and finally obtain the power law for thick screen turbulence:

$$D_\varphi(r) \propto (\epsilon \cdot r)^{5/3} \tag{11.12}$$

For the phase noise ($\Delta\varphi(r) = \sqrt{D_\varphi(r)}$), one has therefore to expect power laws with exponents between 1/3 and 5/6. The absolute scaling factor for the power law and the position of the break where the phase noise levels off depend on the observing site, and of course on the weather.

Due to the quasi-random nature of phase fluctuations, forecasts and inter/extrapolations can be considered inadequate for a phase correction system. Direct measurements of the water vapor column along the line of sight are therefore the most reliable approach.

11.4 Remote sounding techniques

These methods were originally developed for meteorology and control of industrial emissions.

1. **LIDAR**: compares laser back scattering or transmission. DIAL: differential absorption LIDAR, works at two frequencies (on and off the atmospheric line of interest), detects 0.01 g/m^3 water vapor. Disadvantage: works best from aircraft, expensive equipment.
2. **SODAR**: Remote sounding with sound waves. Detects turbulence, but gives little quantitative results.
3. **IR window**: H_2O line absorption in front of a strong continuum source (Sun, Moon, Jupiter). Disadvantage: Directions of observing and monitoring beam differ. The phase correction degrades as a function of the separation angle and the distance of the dominant turbulent layer.

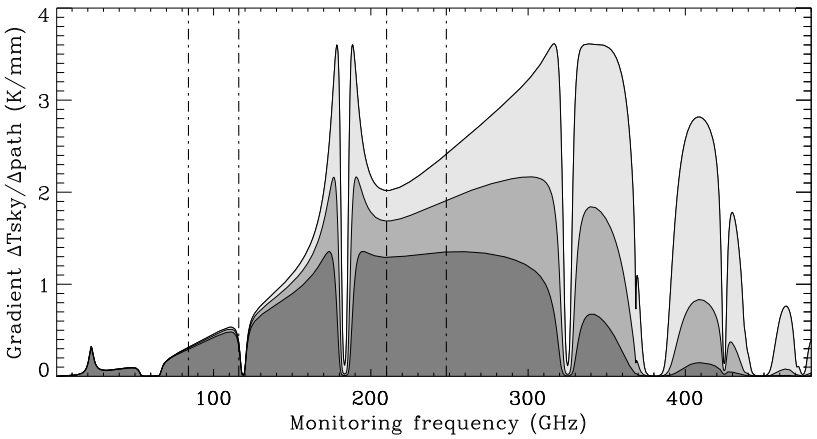

Figure 11.3: Gradient $\Delta T_{sky}/\Delta path$ (K/mm) as a function of frequency and total precipitable water under clear sky conditions. The atmospheric model assumed an ambient temperature of 275 K, pressure 780 mbar, elevation 45°, an observing frequency of 90 GHz and various amounts of water vapor. Light grey: 3 mm water, middle grey: 5 mm water, dark grey: 8 mm water. Dash-dotted lines indicate the receiver tuning ranges of the PdBI.

4. **Radiometric**: Uses the atmospheric emission. Dedicated monitors operate mostly near the 22 GHz or 183 GHz lines (several spectral channels). The inter-line regions of the 1mm and 3mm windows are also sensitive enough, but make it difficult to remove cloud emission.

For the radiometric approach, it is useful to study the sensitivity as a function of frequency, i.e. by how much the sky emission changes for a fixed fluctuation of water vapor, which corresponds to a fixed wet path fluctuation. Fig.11.3 shows what change in T_{sky} one must measure under conditions of various humidity.

There are two reasons to use the 22.2 GHz line: Clouds are easier corrected at this frequency, and receiver components are less expensive.

One notices that the 84-116 GHz window is 1-2 times as sensitive as the 22.2 GHz line, and the 210-248 GHz window 4.5-8.3 times. A dedicated receiver near the 183 GHz water line would have the highest sensitivity, but can suffer from temperature dependent saturation effects. It is better adapted for sites where the total amount of water above the instrument is typically less than 3 mm.

11.5 Current phase correction at IRAM

Remote sounding is done with the astronomical 1mm receivers in the inter-line region at the chosen observing frequency. One uses the total power channel (bandwidth 500 MHz). Advantages of this approach are the close coincidence of observed and monitored line of sight, and the fact that no additional monitoring equipment is needed.

First success was on April 18, 1995, with the installation of the present receiver generation on the PdBI [Bremer 1995]. Critical advantages were the improved total power stability of the receivers and the capability to observe in the 1 mm window. The necessary stability for a 30° phase rms at 230 GHz is about $\Delta M/M = 2 \cdot 10^{-4}$.

Steps of the method:

1. Calibration of the total power counts M_{atm} to T_{sky} as given in the lecture on amplitude and flux calibration.

2. Iterate the amount of precipitable water vapor in an atmospheric model to reproduce T_{sky}. There is no "learning phase" of the algorithm on a quasar, just the model prediction.

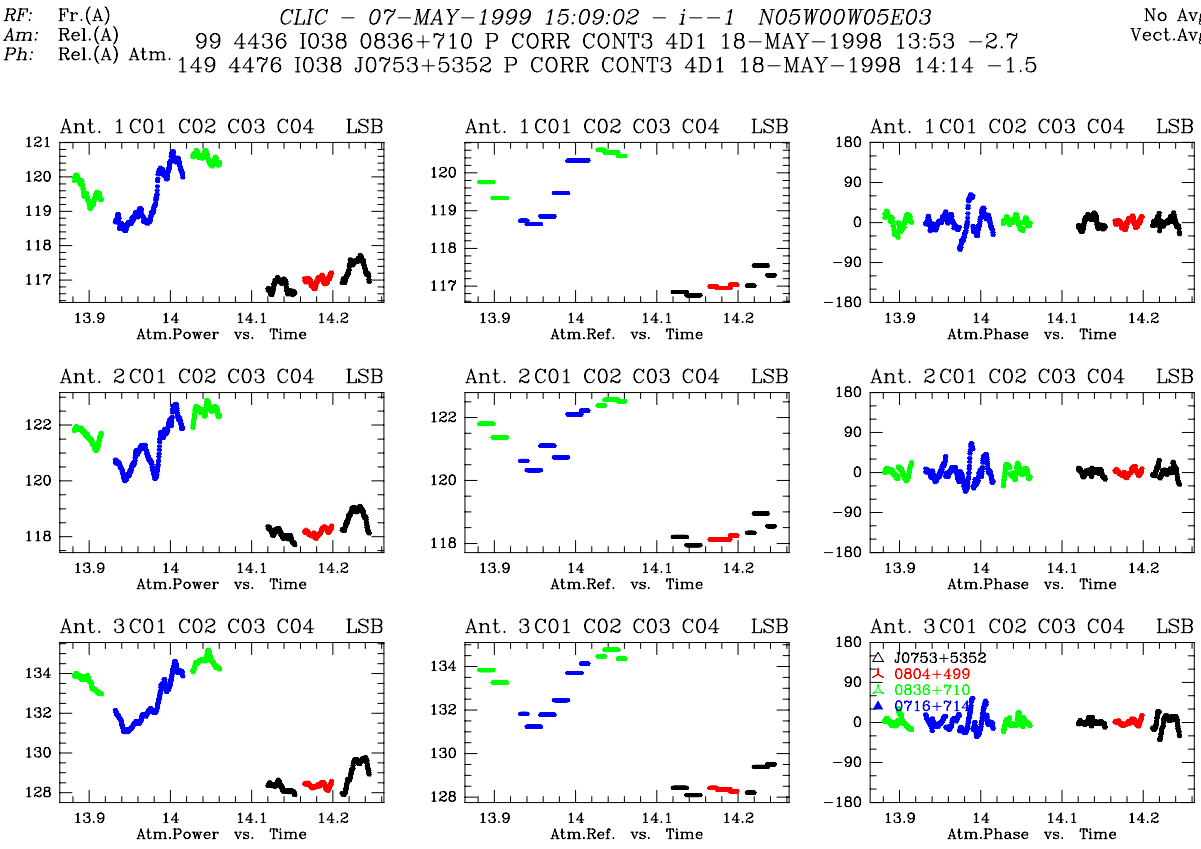

Figure 11.4: Antenna based total power at 228.3 GHz, the reference value to calculate the differential correction, and the model-based phase shift per antenna at 86.2 GHz.

3. The amount of water vapor along the line of sight is proportional to the wet path length.

$$path \approx 6.7 \cdot water(\text{Zenith}) \cdot airmass(\text{Elevation}) \tag{11.13}$$

However, wet path length and opacity have different dependencies on frequency, atmospheric pressure and temperature which should be taken into account. The main increase of the refractive index n of water vapor relative to dry air happens in the infrared, which makes it difficult to use the Cramers-Kronig relations linking it to opacity (integration over many transitions). For simplicity, we use the calculations by [Hill & Cliffort 1981] for the frequency dependency and the temperature and pressure dependencies by [Thayer 1974] instead. These references use not n but the refractivity N, which is defined over the excess path length L relative to vacuum propagation over the line of sight s:

$$L = 10^{-6} \int N_\nu(s) ds \tag{11.14}$$

$$N(P,T) = 77.493 \frac{p_{atm}}{T} - 12.8 \frac{p_V}{T} + 3.776 \times \frac{p_V}{T^2} \tag{11.15}$$

Hill and Cliffort calculate $N(\nu)$ for $T = 300\,\text{K}$, $P = 1013.3\,\text{mbar}$, 80% humidity

$$N(p,T,\nu) = 77.493 \frac{p_{atm}}{T} - 12.8 \frac{p_V}{T} + N(\nu) \frac{p_V}{28.2} \left(\frac{300.}{T} \right)^2 \tag{11.16}$$

4. Subtract the average over a time interval (default: the duration of a scan) to remove residual offsets due to receiver drift and ground pickup, which can be different for each antenna (see Fig.11.4).

5. Convert the antenna specific path shifts into phase at the observed wavelength, $\Delta\phi_i$

6. Calculate the baseline specific phase shifts $\Delta\phi_{ij} = \Delta\phi_i - \Delta\phi_j$. A corrected and an uncorrected version are calculated and stored during the real time reduction which compresses the spectra over one scan. The precision of the correction in relative pathlength is about 65μm per antenna (hence 90μm per baseline, i.e. $\sqrt{2}$ larger).

7. During the off-line data reduction, the user can choose freely between the corrected and uncorrected sets. The phase correction can fail under the following conditions:

   - Clouds: the model only works for clear sky conditions, and will over-estimate the phase shifts seriously in the presence of clouds.
   - Very stable winter conditions: The phase noise of the observations can be below 25° at 230 GHz, which is the intrinsic noise of the correction method.
   - Total power instabilities: For some frequencies, the receivers are difficult to tune. One can get a nice gain in the interferometric amplitude, but an unstable total power signal with an intrinsic noise well above 25° at 230 GHz.

   Even for the cases above, the observer has lost nothing because the uncorrected scans are still there. Software tools are available which help to decide when to apply the correction.

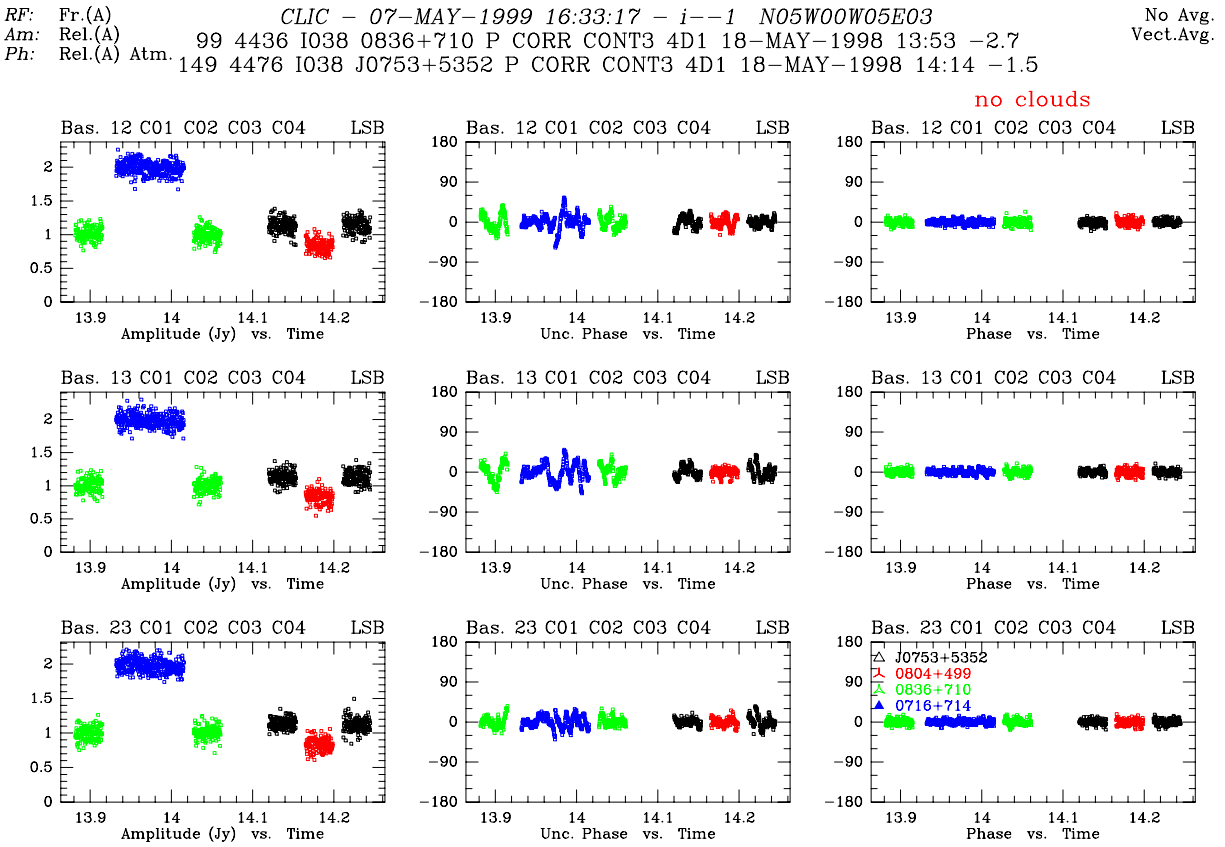

Figure 11.5: Baseline based amplitudes, uncorrected phase and monitor corrected phase at 86.2 GHz with a time resolution of 1 s. The data correspond to the antenna based section in Fig.11.4. The phase calibration applied in columns 2 and 3 was obtained using `STORE PHASE /SELF` on a one minute time scale, thereby setting the mean phases to zero.

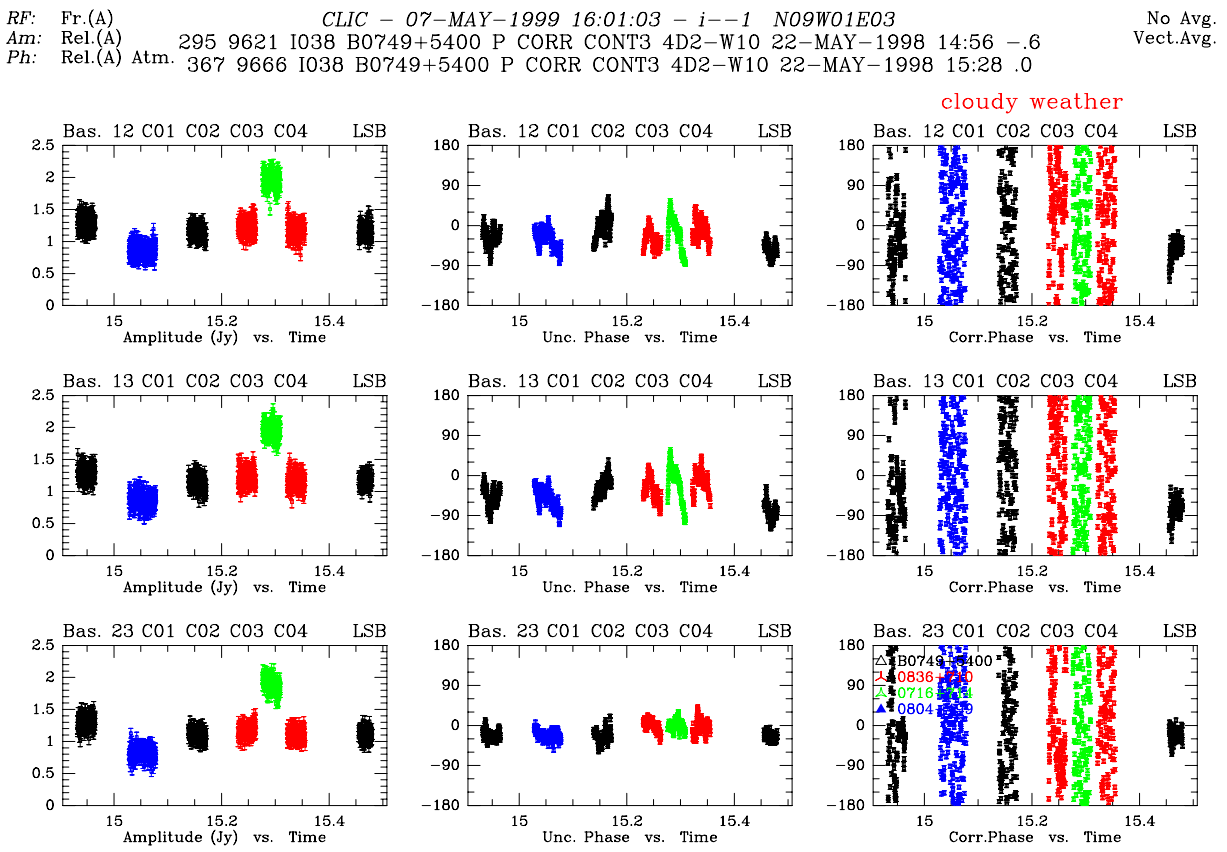

Figure 11.6: Baseline based amplitudes, uncorrected phase and monitor corrected phase at 86.2 GHz for a cloudy data section. The clear sky model over-estimates the correction and would result in serious amplitude loss. The off-line data reduction software will identify those parts and disable the correction there.

11.6 Phase correction during off-line data reduction

In a typical data reduction session, the atmospheric phase correction hides behind two unobtrusive buttons (Fig.11.7). The default of the `PHCOR` button will calculate the phase correction on a scan basis, i.e. only the corrected amplitudes will be used and not the phases. There are two reasons to be cautious about the corrected phases:

- As we have learned from turbulence theory, averages are *not* good in describing data which obey a structure function. Adjusting the monitored phases to zero average can introduce random-like offsets due to slow (large-scale) components of the atmospheric fluctuations. You can only rely on averages if the outer scale of turbulence have passed several times over the instrument. This can be true on your source (typically 20 min integration time), but is doubtful on the calibrators (integrations of typically 3 min). It may work for compact configurations depending on wind speed, i.e. it depends on the weather. There may be an improvement, but it cannot be guaranteed.

- Nearly linear changes in total power can be due to a big water vapor bubble in the atmosphere or a gain drift in the receivers. The first will produce a phase shift, the second will not, and the software cannot tell them apart. In most cases, gain drifts happen when the antenna has just moved a large distance in elevation, as pump friction and liquid helium distribution change with the receiver cabin tilt. Such drifts are invisible in the interferometric amplitude (opacity correction), but the phase correction is more sensitive to them.

The part of related header variables is accessible over
`CLIC> VARIABLES MONITOR`
Some items are scan-based in time resolution, others can be expanded to a time scale of one second over the total power signal. One can plot the following quantities related to the phase correction:

- `ATM_POWER`: total power counts of the monitoring receiver
- `ATM_REFERENCE`: the offsets which are subtracted from `ATM_POWER`
- `ATM_EMISSION`: the calibrated sky emission in Kelvin
- `ATM_PHASE`: the modeled atmospheric phase
- `ATM_UNCORRPH`: the astronomical phase uncorrected from atmosphere
- `ATM_CORRPH`: the astronomical phase corrected with the model
- `ATM_VALIDITY`: 0 or 1 whether the phase correction has been declared valid or not. This flag is antenna specific.

In order to check the validity of the phase correction, the standard reduction runs the command
`CLIC> STORE CORRECTION AUTO 15`
i.e. CLIC will test the phase calibrator observations (type P) if the application of the phase correction improves or degrades the amplitudes, and will declare the correction on source observations (type O) in a ± 15 minutes time window for good.

Apart from `AUTO`, one can use `GOOD` and `BAD` for a manual override of the diagnostics, and `SELF` to check the amplitude for each scan (indifferent to type O or P) for strong sources.

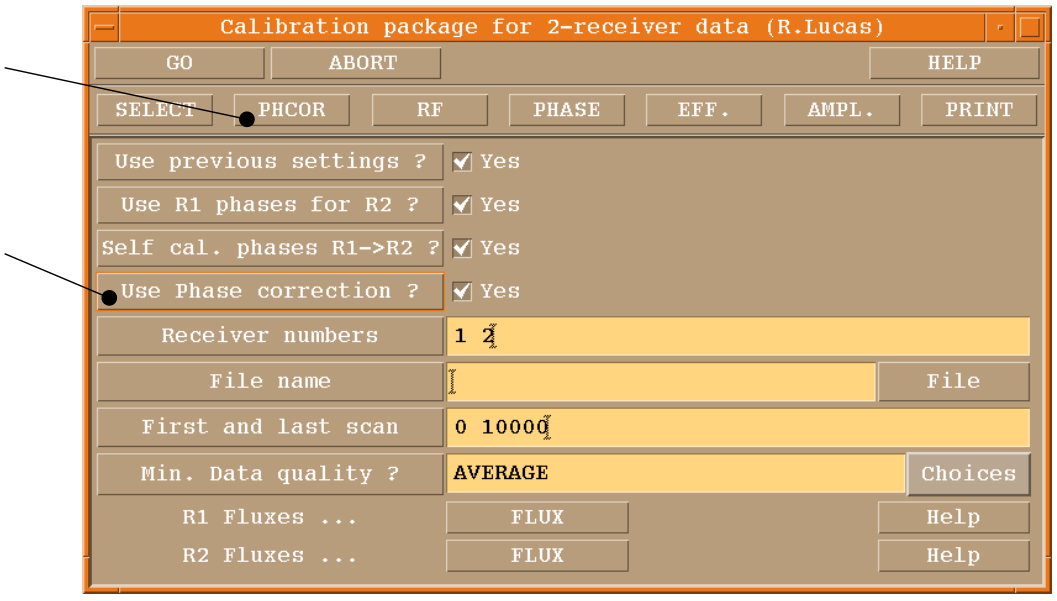

Figure 11.7: The CLIC calibration package menu, with phase correction related items marked.

11.7 Frequently asked questions

- **How often is the phase correction applied?** Statistics have been calculated for all receiver 1 CORR scans in the preliminary data reduction files between September 1997 and March 1999 (a

total of 3120 hours). Over this period, the phase correction was diagnosed "good" during 78.8% of the observing time.

- **Does one gain something on a self calibrated source?** Yes, the monitor corrected spectra are improved on a sub-scan scale, i.e. on one second. An example for this case can be found in Fig. 11.5.
- **How fast can the phase change?** Phases at 3 mm can turn by more than 360° over 30 seconds. Even under calm conditions, it was found that a time resolution of one second for the correction gave better results than an average correction over four seconds.
- **Is dry weather the same as low phase noise weather?** Unfortunately not. Even with 3mm precipitable water, one can have very bad phases if the wind is high (about 10 m/s).
- **Why is the phase correction sometimes disabled under clear sky conditions?** Each correction system has its intrinsic noise. If the atmospheric phase noise is below 10° at 3 mm or 30° at 230 GHz (which happens under stable winter conditions), the added noise will undo the benefits, and the diagnostics will switch the correction off. The same can happen under less favorable conditions if a receiver has an unstable total power signal (this can happen at some frequencies).
- **How does the corrected phase depend on baseline length?** Basically, it becomes independent. Over time scales longer than the monitor time interval, the structure function dependence stays.
- **Are there still changes / improvements in the system?** Yes, we are working on it.